Desalination and Water Treatment
www.deswater.com

doi: 10.5004/dwt.2017.20156

64 (2017) 136–146
February

Lab-scale experiment assessment of air sparging BTEX removal in fine-grained aquifer of Shiraz Oil Refinery

Hamidreza Heidari[a], Mohammad Zare[a,*], Jim F. Barker[b], Abdorreza Vaezihir[c]

[a]*Department of Earth Sciences, Shiraz University, Shiraz, Iran, Tel. +98 7136137473; Fax: +98 7132284572; emails: hamidreza.heidari.s@gmail.com (H. Heidari), zare@susc.ac.ir (M. Zare)*
[b]*Department of Earth and Environmental Sciences, University of Waterloo, Waterloo, Ontario, Canada, email: jfbarker@uwaterloo.ca*
[c]*Department of Earth Sciences, University of Tabriz, Tabriz, Iran, email: r.vaezi@tabrizu.ac.ir*

Received 23 January 2016; Accepted 11 August 2016

ABSTRACT

Groundwater contamination by petroleum hydrocarbons is a major concern throughout the world. Shiraz Oil Refinery (SOR) site has been subjected to several leakage and spills in the past, and consequently six separate non-aqueous phase liquids sources and their consequent plumes are formed in the fine-grained Quaternary aquifer of the site. Laboratory experiments were performed to study the benzene, toluene, ethyl-benzene, and the three xylene isomers (termed BTEX) removal efficiency of air sparging (AS) method, using a site porous material in a three-dimensional flow box model. Different air injection flow rate and injection patterns in four different set of experiments were examined. Water level change (upwelling), dissolved oxygen (DO) values as indirect indicator of sparging well radius of influence (ROI) and BTEX concentration of the saturated zone as direct indicator were measured in a dense network of monitoring wells installed in the porous material section. Results showed that channelized airflow is more probable, resulting in reduction of the effectiveness of the AS in the SOR fine-grained aquifer. To apply AS method in this media, decreasing AS flow rate but increasing sparging points is a more efficient strategy during AS operation. Furthermore, special consideration should be taken in determining ROI in fine-grained porous material due to channelization of airflow. Therefore, a proper design of number and placement of the sparging points and monitoring wells are required. Therefore, AS remediation method is effective to reduce BTEX concentration in fine-grained material of SOR aquifer if well designed and operated.

Keywords: Groundwater contamination; Air sparging; BTEX remediation; Zone of influence; Radius of influence; Shiraz Oil Refinery

1. Introduction

Groundwater contamination by light non-aqueous phase liquids (LNAPLs), due to leakage and spills of petroleum hydrocarbons from storage tanks, pipes and drains in refineries, gas stations, and elsewhere is a major concern throughout the world [1]. More soluble compounds of these chemicals especially benzene, toluene, ethyl-benzene, and the three xylene isomers (termed BTEX) and oxygenates such as methyl-tertiary butyl ether (MTBE) are easily dissolved and transferred into groundwater and subsequently to downstream water resources. BTEX compounds have also relatively high vapor pressures, which is a measure of their tendency to partition from the LNAPL into the gaseous phase. These volatile organic compounds (VOCs) pose a significant risk to human health and environment even at very low concentration [2]. Therefore, remediation of contaminated sites with these compounds is crucial. In situ air sparging (IAS) is one of the most efficient techniques to remedy the saturated soils and groundwater contaminated with VOCs [3–9]. The technology involves the injection of contaminant-free air into the subsurface saturated zone to partition the free phase trapped in the soil pores and dissolved VOCs of the saturation and capillary zones into

* Corresponding author.

vapor phase. In this technology, air is injected into or below the contaminated zone of aquifer; the airflow through the aquifer results in the volatilization of VOCs from the non-aqueous or aqueous phase to the gas phase. Through this process, also oxygen is transferred from air to the contaminated groundwater, which in turn may promote biodegradation of VOCs [10].

Before implementation of an in situ groundwater remediation system at a site, treatability testing should be performed to verify the effectiveness of proposed remedial approach and to develop site-specific design criteria and operating conditions [11]. Treatability testing can be performed in two phases: bench-scale and pilot-scale testing. Bench-scale tests are conducted in the laboratory to evaluate the effectiveness of a process, while pilot-scale tests simulate full-scale operations in the field to gain some full-scale design parameter according to site specification.

Complex processes occur during the operation of an air sparging (AS) system that have effect on AS design, installation and operation. Numerous laboratory investigations of AS systems, mostly one- or two-dimensional scale, have been conducted to gain understanding of these processes. Most of these studies focused on the factors and system parameters influencing removal efficiency [12–23].

The most important parameter in evaluation of an AS system design is determination of the radius of influence (ROI) of the sparging wells and the zone of influence (ZOI) of the system. The nature and extent of airflow during AS determine the ZOI and contaminant removal efficiency. The mode of the air migration (bubble or channel flow) in the aquifer material is an effecting process on ROI. ROI can be determined by indirect and direct indicators. Four commonly used indirect indicators to estimate the ROI of sparging wells are: measuring the pressure response below the water table, dissolved oxygen (DO) concentration in the ground water, measurement of groundwater mounding (upwelling), and increase in VOC vapor concentration in the unsaturated zone [24–28]. Direct indicator of the ROI is measuring the decreasing rate of the concentration of the contaminant (contaminant removal) by analyzing the water samples taken from the monitoring wells during the operation period. The ROI of the sparging well is difficult to determine. However, the zone at which contaminant removal occurs (contaminant cleanup zone) best defines the sparging well ROI.

Researchers described airflow during AS process according to air-water two-phase flow theory. Gao et al. [29] discussed the transition criteria between two flow patterns observed during AS tests, bubbly flow and channelized flow, according to two-phase flow theory. Gao et al. [30] was performed micromechanical investigation to understand the physics of air migration and subsequent spatial distribution of air at pore scale during AS.

Recently, the centrifuge technique was employed to investigate the mechanism of AS under in situ stress state condition. Hu et al. [31] were performed centrifugal modeling tests to investigate airflow rates and the evolution of the ZOI during the AS under various gravity acceleration levels, g levels. Hu et al. [32] investigated the flow pattern transition during centrifugal tests under different g levels and studied the scaling factor for ZOI during centrifugal tests. Most of the laboratory experiments conducted in one- or two-dimensional soil columns and a limited number of experimental studies have been conducted on evaluating BTEX remediation process by AS under three-dimensional flow conditions. However, although numerous laboratory studies and field applications indicate the effectiveness of AS method, but site specification (i.e., site material and hydrogeology) causes fundamental limitations associated with the efficiency of this technology. A proper design and installation of AS to achieve remedial goals require gaining information on complex processes, which occur during the operation according to each site-specific condition. While field studies is complicated and expensive and gaining information on specific mechanisms of AS in the site is difficult, small-scale laboratory model experiments as a preliminary study prior to the field-scale work can help in evaluating the technology effectiveness and to gain information on some specific processes, which occur during AS based on that site specific conditions.

Shiraz Oil Refinery (SOR) site has been subjected to several leakage and spills in the past. Preliminary studies found two LNAPL source areas at the site [33]. Vaezihir et al. [34] differentiated six separate LNAPL sources and their consequent plumes. A three-dimensional numerical flow and transport model was applied by them to simulate the fate and transport of BTEX from these source zones of LNAPLs. Results showed that all of the down-gradient pumping wells are at risk of being contaminated by BTEX in the future under natural conditions, and enhanced remediation (ER) is recommended to reduce the risk of contamination of the present drinking water wells located down-gradient [34].

The present study is designed to evaluate the BTEX removal efficiency by AS in the SOR aquifer. Different air injection flow rate and sparging point patterns are examined in a lab-scale three-dimensional flow box model using the site's fine-grained porous materials.

1.1. Site description

The SOR is located northeast of the city of Shiraz, Islamic Republic of Iran. The SOR site occupies an area of 2.3×10^6 m^2 with an annual production capacity of 3 million metric tons of product including diesel, gasoline, fuel oil, kerosene and liquid petroleum gas (LPG).

The SOR is surrounded by massive limestone, which is karstified and supports a number of drinking water wells located about 2,200 m from the site, supplying water for the Shiraz municipality. In addition, several irrigation and local drinking water alluvial wells are also located downstream of the site (the closest of which is about 700 m away). Further information about the site is available in Vaezihir et al. [34].

The Quaternary aquifer at the SOR site is about 25 m thick consists of fine grain sand and silty material over lying by marly layer considered as bedrock. Depth to groundwater ranges from 5 to 17 m, and the hydraulic conductivity is in the range of 2.5×10^{-6}–2.1×10^{-5} m/s [34]. The general flow direction is from west to east across the site. The average hydraulic gradient estimated using the water table elevation is about 0.017. The aquifer is recharged by rainfall and inflow from the western karstic limestone formations.

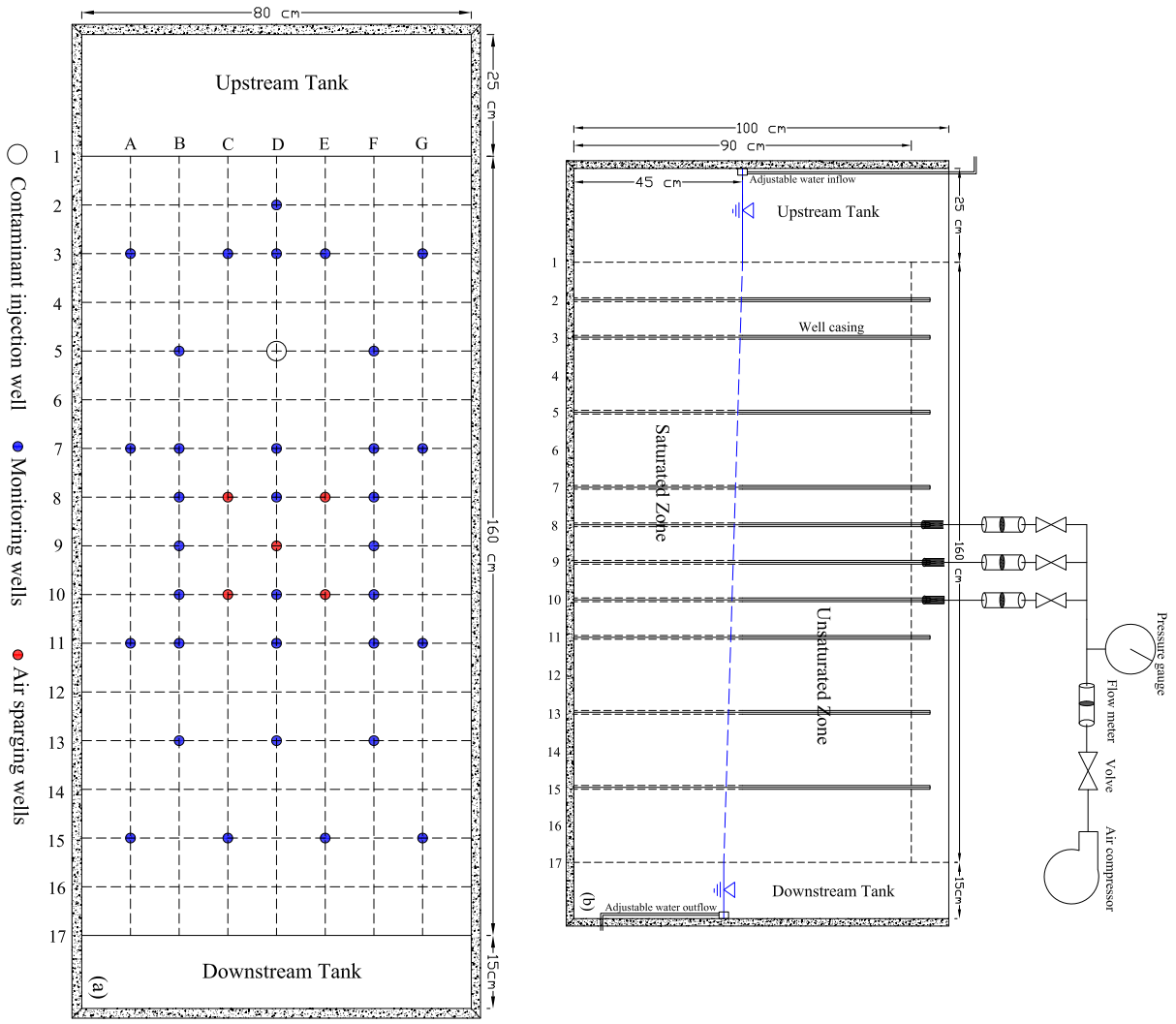

Fig. 1. Schematic of flow box model: (a) plan view, (b) side view, observing the monitoring wells of row A and B in Fig. 1(a).

2. Methods and material

2.1. Laboratory setup

2.1.1. Box installation

The experiments were conducted in a three-dimensional laboratory-scale box model made of glass walls supported by an aluminium frame. The inner dimensions of the container were 2.0 m × 0.8 m × 1.0 m, which was separated into three sections: an upstream and a downstream part to contain only inflow and outflow water and a porous material container in the middle (Fig. 1). The middle section was filled with well-drilled site porous material, which carefully was placed in the tank homogeneously.

Partitioning was done with perforated screen walls covered with fiber glass plankton net to prevent porous material from entering into the water tanks. The soil material was added to a total height of 0.9 m. A 0.03-m thick clay material was used in contact with the glass walls to prevent preferential flow of water and injecting air during the experiments. The saturated zone was separated from the unsaturated zone by a 0.05-m thick fine-grained gravel to minimize capillary rise. Following soil placement, the soil profile was gradually saturated from the bottom to a height of 0.45 m by introducing water into the upstream tank. The system was left idle for days to gain a steady condition.

2.1.2. Air injection and sampling wells

Thirty-eight wells including five AS wells and thirty-three monitoring wells as measurement and sampling points using perforated PVC pipe each 0.02 m in diameter were installed in the porous material section. The wells are named according to their grid coordinate of the box model, which is shown in Fig. 1(a). The sparging wells were screened from 0.1 to 0.35 m below water level in the saturated zone. The monitoring wells were continuously screened through the entire saturated zone. Pipes were wrapped with fiber glass plankton net to prevent porous material entering the wells. Sparging wells were surrounded by a fine-grained gravel pack used as filter and then

were sealed above the water table with bentonite to prevent air from short-circuiting to the surface. Each well includes a thin elastic Tygon tube and a syringe for taking water samples.

Upstream and downstream tanks helped to control inflow and outflow rates in the aquifer by the means of adjusting the water level and consequently hydraulic gradient of the system. The upstream tank was connected to a tap water of a tank with a constant head to create a uniform flow. The downstream tank water level was controlled using an adjustable overflow system. AS was simulated by introduction of air provided by an oil-free air compressor. A control panel consisting of a pressure regulator, pressure gauge, flow meter and valves used to verify the proper air pressure and flow rate throughout testing (Fig. 1(b)).

2.2. Soil material

The properties of the soil material are presented in Table 1.

2.3. Experiments

Four different sets of AS experiments were conducted. In each experiment, a steady-state groundwater flow conditions were enforced. The horizontal hydraulic gradient was set at 0.018, similar to that of the SOR aquifer, by controlling water levels at 45 and 42 cm above the base of the model in the upstream and downstream water tanks, respectively. The outflow rate was set at the 38.6 cm^3/min (with an average groundwater flow velocity of 0.011 cm/min), which was checked regularly and held constant during all experiments. A pressure of 5–8 KPa over atmospheric pressure was applied to induce air into the subsurface during sparging periods.

During the experiments, an oil/water interface probe (Heron Instrument Company, model H.oil; Ontario, Canada) with 1 mm accuracy was used to measure the water depth and LNAPL thickness. DO was measured with a DO meter type SensION6 supplied by Hach Company, USA. Water samples were analyzed for BTEX concentration in the environment laboratory of Iranian Mineral Processing Research Center (IMPRC) through gas chromatography using a chromatograph (model 6890, Agilent, USA) equipped with a mass selective detector (model 5975, Agilent, American). The packed column used was a model HP-5 (30 m × 25 mm, 0.25 μm Agilent Technologies, Santa Clara, California). The injector and detector were set at 210°C and 250°C, respectively. The column operated from 40°C (5 min hold), then to 80°C at a speed of 6°C/min. The carrier gas was He at 1 cm^3/min, and the split ratio was 2:1. The grain size distribution analyses were determined using the ASTM D422-63 sieving method. The hydraulic conductivity of porous material was estimated using the constant head method and steady-state flow condition using the box model.

Table 1
Properties of the porous material used in experiments

Parameter	Value
Bulk density, ρ_b (kg/m^3)	1,810
Effective grain size, D_{10} (mm)	0.06
Medium grain size, D_{50} (mm)	0.2
Uniformity coefficient, U (D_{60}/D_{10})	5
Porosity, N	0.37
Hydraulic conductivity, K (cm/min)	0.6
Org. C, f_{oc} (%)	0.1

2.3.1. Experiment no. 1 (EX1)

Air was injected into the saturated zone through an AS well placed on the centre line of the model (D9 in Fig. 1(a)) continuously with a flow rate of $(10 \pm 1) \times 10^3$ cm^3/min for 24 h (experiment EX1-1), and then increased to $(20 \pm 1) \times 10^3$ cm^3/min for the next 24 h (experiment EX1-2). DO and water level in all other wells (Fig. 1(a)) were measured before and during the sparging period at different time intervals to evaluate the ZOI and migration and distribution of airflow through different sparging strategies. After 48 h, the air injection was terminated.

2.3.2. Experiment no 2 (EX2)

In the second set of experiments, in the beginning, the water level in the downstream tank was lowered gradually to the base of the aquifer to drain and washout the oxygenated water. Water level was raised and lowered several times within several days to completely wash out the oxygenated water and replace fresh tap water from upstream tank, and minimize the accumulation of air trapped in the saturation zone during the EX1. Afterward, a steady-state groundwater flow condition was enforced again using a horizontal hydraulic gradient the same as in EX1. Air was injected into the saturated zone through five AS wells: C8, E8, D9, C10 and E10 (Fig. 1(a)). Air was injected at a flow rate of $(6 \pm 1) \times 10^3$ cm^3/min in each well for 24 h. DO and water level in all other wells located within the aquifer chamber were measured before and during the sparging period in different time intervals.

2.3.3. Experiment no. 3 (EX3)

After preparing the box model as described in EX2, 120 cm^3 of unleaded gasoline was injected through contaminant injection well, D5 (Fig. 1(a)). The contaminant injection well was a PVC pipe with the internal diameter of 4 cm. Gasoline was injected on the water table, using a 60 cm^3 syringe fitted with thin elastic Tygon tube with the average injection flow rate of 6 cm^3/min. After 6 d, continuous AS at well D9 started, initially with a flow rate of $(10 \pm 1) \times 10^3$ cm^3/min for 24 h (experiment EX3-1) then $(20 \pm 1) \times 10^3$ cm^3/min for the next 24 h (experiment EX3-2). Water samples were collected for BTEX analysis before starting and during sparging periods in all other wells at different time intervals. Water samples were collected into amber glass vials with Teflon-lined screw caps, avoiding air bubbles in the sample, and the vials were wrapped with parafilm. The syringes and the thin Tygon tubes were allocated for every well. Samples were spiked with a bacteriastat (0.4 cm^3 of a 10% w/v sodium azide solution), placed in a refrigerator at 4°C–6°C not longer than 2 weeks before analysis.

2.3.4. Experiment no. 4 (EX4)

For this experiment, after initial preparation works including trying to remove any gasoline remained from the

Table 2
Summary of four different set of AS experiments

Experiments		Sparging well	Sparging flow rate in each well (cm^3/min)	Sparging duration (h)	Measured parameters	Experiments objective
EX1	EX1-1	D9	$(10 \pm 1) \times 10^3$	24	DO and WL	Evaluating sparging ZOI through different sparging flow rate
	EX1-2	D9	$(20 \pm 1) \times 10^3$	24 (next 24 h of ending EX1-1)		
EX2		C8, E8, D9, C10, E10	$(6 \pm 1) \times 10^3$	24	DO and WL	Evaluating sparging ZOI during change in sparging strategy
EX3	EX3-1	D9	$(10 \pm 1) \times 10^3$	24	BTEX	Evaluating BTEX removal efficiency and sparging ZOI through different sparging flow rate
	EX3-2	D9	$(20 \pm 1) \times 10^3$	24 (next 24 h of ending EX3-1)		
EX4		C8, E8, D9, C10, E10	$(6 \pm 1) \times 10^3$	24	BTEX	Evaluating BTEX removal efficiency and sparging ZOI during change in sparging strategy

previous experiment and washing the material by raising and lowering water table for many times during days, the system was made ready for the EX4.

In this experiment, again 120 cm^3 of unleaded gasoline was injected in well D5, and after 6 d, AS was initiated through five injection wells (C8, E8, D9, C10 and E10) with flow rate of $(6 \pm 1) \times 10^3$ cm^3/min in each well for 24 h. Water samples were collected before and during sparging periods for BTEX analysis as explained in EX3. These experiments are summarized in Table 2.

3. Results and discussion

To evaluate the BTEX removal efficiency of AS in the fine-grained aquifer of SOR before implementation of an in situ operation at the site, as main objective of this study, lab-scale AS treatability testing is performed by a series of tests. DO, water-level change (upwelling) and BTEX concentration analysis as indirect and direct indicators of ROI were considered for evaluation.

3.1. DO measurements

The changes of DO value of pore water during AS are related to the air saturation. Therefore, the distribution of DO concentration in the groundwater and its change during AS is used to evaluate the sparging ZOI during the AS operation. The DO value in wells recorded before the operation is considered as the background value, and its change during the operation is considered as ΔDO.

Fig. 2 shows the change of ΔDO during EX1 in the wells that were affected by induced air. This figure demonstrates that during sparging with $(10 \pm 1) \times 10^3$ cm^3/min through one injection well in EX1-1, ΔDO increased for the first 4 h and stayed constant for up to 24 h when the sparge rate was increased to $(20 \pm 1) \times 10^3$ cm^3/min (EX1-2). There again ΔDO value increased in the first 3 h and continued with no significant changes up to the end of EX1-2. Wells, which didn't show significant changes during EX1-1 (C8, F8 and E10), although some of them have lower distance to sparging point respect to those affected, were affected during EX1-2, and their ΔDO increased as did the other

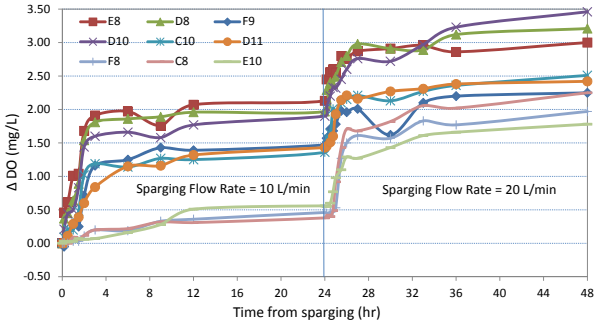

Fig. 2. DO value change (ΔDO) with time in wells affected by induced air during EX1 operation.

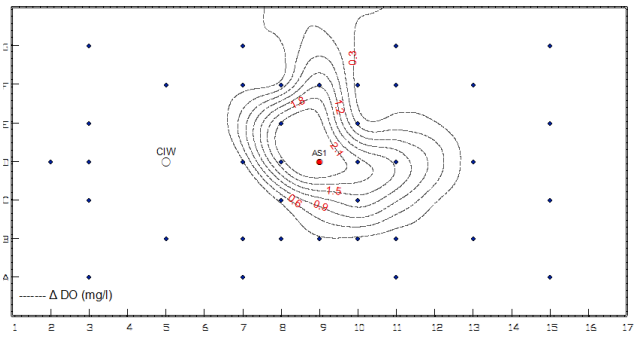

Fig. 3. Contour map of DO value change (ΔDO) in groundwater at the end of EX1-1 operation (24 h after air injection with flow rate of $(10 \pm 1) \times 10^3$ cm^3/min).

wells. This is probably because of opening additional channels during EX1-2 with higher injection flow rate. The maximum distance affected from the sparging point in EX1-1 and EX1-2 is 20 and 22.4 cm, respectively. In consequence, doubling the flow rate did not cause significant increase in the sparging well ROI, although caused higher DO concentration and more affected wells because of increased channel flow density.

Contour map of ΔDO at the end of the EX1-1 and EX1-2 are presented in Figs. 3 and 4, respectively. According to these figures, the internal area of iso-DO value change, (contour of

ΔDO = 1.0, e.g., that we chose as significant DO value change) for Figs. 3 and 4 are 135 and 170 cm^2, respectively. Therefore, the extent of the ZOI for EX1-2 is not significantly larger than that of EX1-1. However, the DO value of the ZOI for EX1-2 is increased. Apart from this, the figures show that the ZOI is not symmetrical around the sparging point and have elongated toward the north and west (in the figures). This situation might because of channelized airflow in the system in some directions. Although extending the ZOI toward the west might be due to the groundwater flow direction. This situation results in ambiguity of definition of each sparging wells ROI.

The EX2 ((6 ± 1) × 10^3 cm^3/min in five wells) DO measurements in the affected wells are also presented as ΔDO values with time in Fig. 5. The number of the affected wells and their ΔDO are greater than in EX1. The trend of increasing ΔDO in the affected wells is similar to that of EX1, although they stabilized with a higher ΔDO values and in a shorter time.

Fig. 6 shows the contour map of ΔDO for the end of EX2. Decrease in sparging flow rate of each well but increase in the number of sparging points caused more uniform air distribution and developed a broader sparging ZOI in the aquifer with higher DO compared with EX1. Unlike EX1, in this experiment, all the wells located in the ZOI limit affected by induced air. It seems that, when sparging flow rate reduces, induced air migration is limited to shorter distance around the sparging point, and more bobble flow is formed as opposed to channelization. Or probably channels developing from adjacent points likely overlap to some extent, increasing the density of channels.

3.2. Upwelling

During the sparging operation, water level begins to rise above the original water level (termed as upwelling) for some time, and it is lower afterward. If upwelling dissipated faster, channelized airflow is more probable flow mode, while if it remained during sparging operation bubbling is more probable flow mode [35,36].

Water level measurements were conducted before and during AS experiments operation in monitoring wells located in the porous media. The water level change in affected wells during EX1 operation is depicted in Fig. 7. In some wells around the sparging point, water level begins to rise with starting of AS and increased sharply, reaching a peak in about 20 min and then lowered to almost original water level in 4 h. For EX1-2, the rise is bigger, and it lowered, but not to the original water level. This may be due to the higher pressure and induced airflow rate and probably opening more channels.

Fig. 8 shows water level rise during EX2 operation only for those wells not responded in EX1 for comparison with Fig. 7. However, more wells and in result larger area is affected in EX2 due to more injection points and along with it higher total injecting flow. Upwelling remained longer during sparging operation in EX2, unlike the EX1 that there was more transient and dissipated in almost first 3–4 h

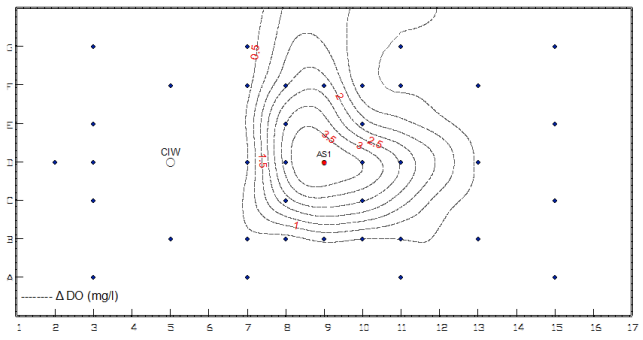

Fig. 4. Contour map of DO value change (ΔDO) in groundwater at the end of EX1-2 operation (24 h after air injection with flow rate of (20 ± 1) × 10^3 cm^3/min).

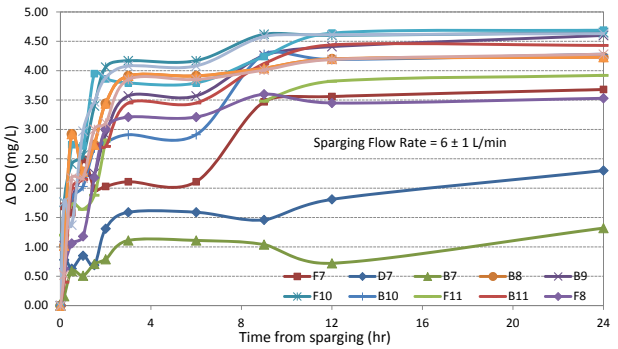

Fig. 5. DO value change (ΔDO) with time in wells affected by induced air during EX2 operation (injection points = 5 wells, flow rate = (6 ± 1) × 10^3 cm^3/min).

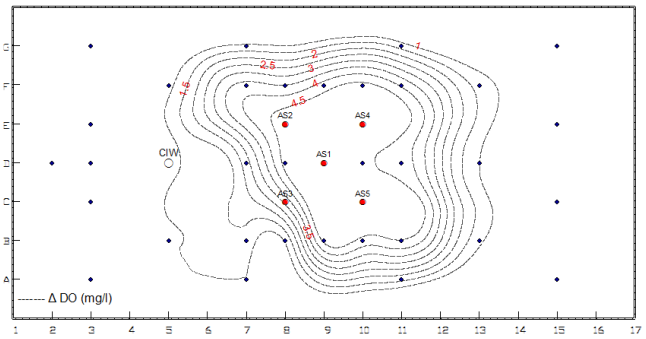

Fig. 6. Contour map of DO value change (ΔDO) in groundwater at the end of EX2 operation (after 24 h of air sparging through 5 sparging wells, air injection flow rate = (6 ± 1) × 10^3 cm^3/min).

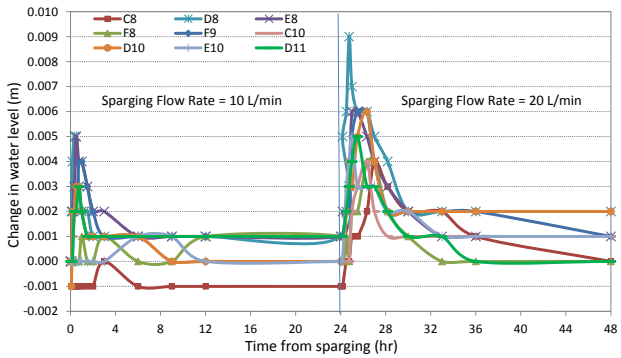

Fig. 7. Water level change with time in wells affected by induced air during EX1 operation.

of sparging. Comparing Figs. 7 and 8 indicates that during EX1 more than 75% of upwelling dissipated in first 3 h of sparging and almost 90%–95% of initial upwelling dissipated in 8 h. Whereas during EX2, almost 50% of initial upwelling dissipated in first 3 h of sparging; about 75% of initial upwelling dissipated in 8 h; and about 25% of initial upwelling remained during sparging operation. The rise and decay of water mound may reveals that unlike the EX1, channelling phenomenon is less for EX2 and more bubbling airflow is happening in closer distance around each sparging well.

3.3. BTEX measurements

In EX3, BTEX components of gasoline injected into the well D5 (as contaminant source) dissolved in groundwater and generated a BTEX plume within the aquifer area. The AS experiment was initiated 6 d after gasoline injection. The sum of the BTEX compounds concentration was considered rather than individual compounds, and BTEX removal efficiency and AS wells ROI was evaluated through BTEX concentration analysis as a direct indicator of ROI. In order to compare the results over time, the ratio of sum of the BTEX concentration measurements for any point and any time during the AS operation (C) to the initial concentration at each point before sparging (C_0), called as relative concentration (C/C_0), used for indicating BTEX removal progresses in each time intervals during AS experiments.

Fig. 9 shows C/C_0 variation in the sampling wells that have significant change during the operation in EX3 (sparging at (10 ± 1) × 10^3 and (20 ± 1) × 10^3 cm^3/min in well D9). Other wells not showed significant change in BTEX concentration. This figure shows that total BTEX concentration in wells D8, E8, F9, C10, D10 and D11 in different locations was reduced about 40%–80%, in the first 6 h of air injection during EX3-1. Afterward, the concentration did not decrease remarkably until the end of this experiment. When EX3-2 started immediately more BTEX removal happened in the same wells again for the first 6 h and C/C_0 reached to a constant level of about 0.2 (Fig. 9). Furthermore, this figure indicate that BTEX removal in the wells F8, C8 and E10 that initially were about 10%–30% during EX3-1, although some of them have lower distance to sparging point respect to those with significant BTEX removal, increased during EX3-2 due to increase of sparging flow rate and probably increased channel density. The result of this experiment as shown in Fig. 9 indicates that BTEX removal rates in the sampling wells were not proportional to their distance from the sparging point. This must reflect channelized airflow in the saturated porous media. Airflow occurring in discrete, stable channels is the most probable flow behavior in the medium to fine-grained porous media [12,37]. Since the water in contact with the air channel is the only location where VOCs and air are in direct contact, VOC volatilization occurs in air channels. For contaminants out of air channels, there is a diffusion limitation to volatilize into the air channels. Therefore, the groundwater at a distance from the air channel can be quite high in VOC content; however, the water at the air channel (air/water interface) will have reduced VOC content. This also results an ambiguity to define the sparging well ROI through analyzing a direct indicator of ROI (BTEX removal analysis) in the porous media.

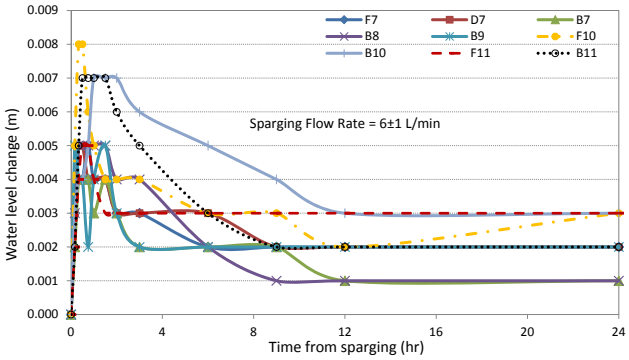

Fig. 8. Water level change with time in wells affected by induced air during EX2 operation.

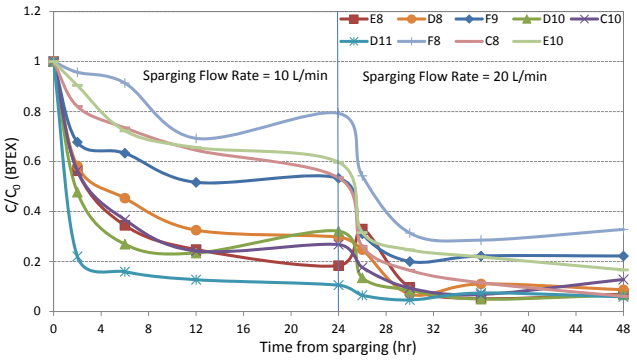

Fig. 9. Relative BTEX concentration, C/C_0, in sampling wells with elapsed time during EX3 operation (C_0: initial BTEX concentration).

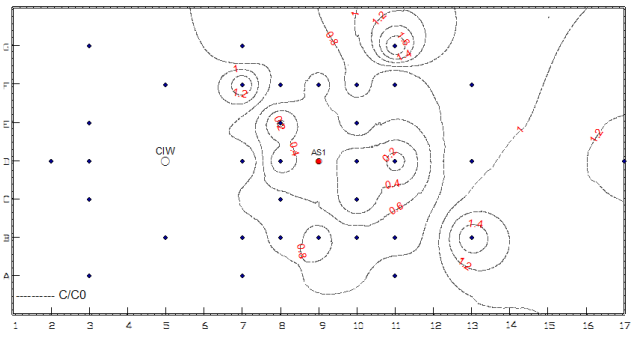

Fig. 10. Contour map of relative BTEX concentration (C/C_0) at the end of EX3-1 operation.

To further examine the extent of the remediation efficiency, a contour map of relative BTEX concentration (C/C_0) for the end of EX3-1 operation is presented in Fig. 10. Contours show that significant decrease in BTEX concentration has occurred after 24 h, but the removal is not symmetrical around the sparging point. Also, some areas nearer to the sparging point showed less BTEX removal in comparison with areas at a greater distance from the sparging point. Of interest, downstream of the sparging point (see Fig. 10), the relative BTEX concentration (C/C_0) is greater than unity. This might reflect not affected area contaminants migration toward downstream or limitations of discretizing the space and time domains of a temporally variable plume.

Contour map of C/C_0 for the end of EX3-2 is shown in Fig. 11. Comparing Figs. 10 and 11 suggests that increasing the sparging flow rate has caused greater BTEX removal with development of a larger ZOI. However, as this figure also shows wells with same distance from sparging point did not show a same BTEX removal rate. In addition, away from the ZOI and in the downstream direction after 48 h, concentration of BTEX has become greater than unity as observed in EX3-1.

Comparing sampling wells BTEX removal results indicate that increasing sparging flow rate not caused significant increase in sparging well ROI. Well at maximum distance of 20 cm from sparging point had significant BTEX removal rate during EX3-1, while with increasing sparging flow rate to (20 ± 1) × 10^3 cm^3/min well at maximum distance of 22.4 cm from sparging point had significant BTEX removal rate. Comparing Figs. 10 and 11, the internal area of iso-contaminant removal, C/C_0, (contour of C/C_0 = 0.6, e.g., that we chose as significant BTEX removal level) for Figs. 10 and 11 are 149 and 182 cm^2, respectively. Therefore, again doubling the sparging flow rate did not cause significant increase in sparging well ZOI. But probably because of increase of channelized flow density due to increase in sparging flow rate more wells in the ZOI showed significant BTEX removal and higher BTEX removal happened during EX3-2.

In the EX4 operation, BTEX analysis results of the sampling wells are shown in Fig. 12 as C/C_0 vs. time from sparging. This figure shows that more BTEX removal has happened in the sampling wells in the first 6 h of AS operation, and after which this rate has decreased. The final C/C_0 reached to about 0.2–0.4. An increase in BTEX concentration, i.e., C/C_0 higher than unity in the first hours of operation, is also depicted from Fig. 12 in some sampling wells. This might be in result of pore water replacement with higher contamination level due to formation of air channels. In this experiment, also BTEX removal rate has increased in comparison with EX3. This figure also shows that the number of the influenced wells have increased resulting in the expansion of the ZOI.

Contour map of relative BTEX concentration for end of EX4 operation is shown in Fig. 13. Considering the condition of this experiment, decrease in sparging flow rate of each well but increasing number of sparging point in the same time and along with it increase of volume of induced air have caused an increase of BTEX removal with extended ZOI in comparison with EX3. In this operation, the ZOI has expanded in all direction with a better uniformity. In contrary to the results of EX3, increase in the C/C_0 is not observed in downstream. Overall, the EX4 produced better results in removal of the BTEX. Therefore, when channelling is a removal rate-limiting factor and reduces AS effectiveness in fine-grained material, one may thought that AS remediation technology is not effective in SOR aquifer because of fine-grained porous material of aquifer, but results of study indicate that by some considerations such as decreasing airflow rate and increasing number of spaging points, this limitation could be relaxed and increases AS range of applicability in fine-grained porous material. Also results of study indicated that because of channelling phenomena during AS in the fine-grained porous material, monitoring well location is effective in estimating of sparging well ROI and special consideration in determining ROI is required by proper design of number and placement of monitoring points.

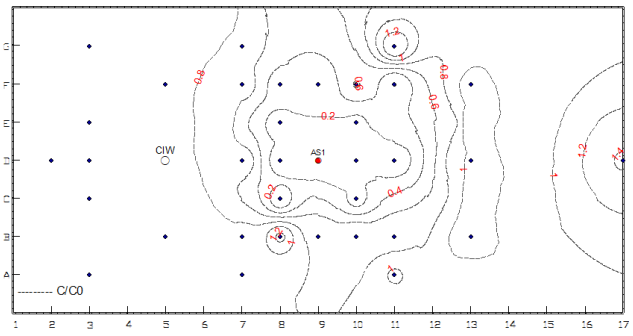

Fig. 11. Contour map of relative BTEX concentration (C/C_0) at the end of EX3-2 operation.

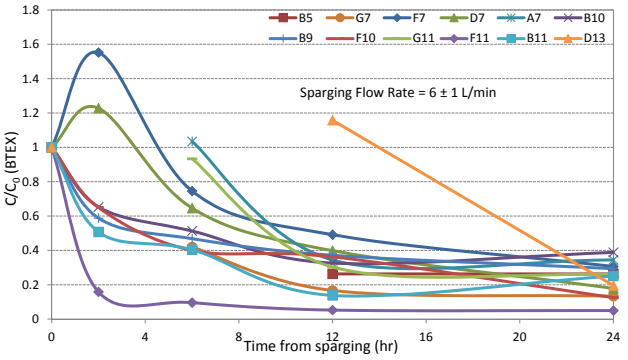

Fig. 12. Relative BTEX concentration, C/C_0, in sampling wells with elapsed time during EX4 operation. (C_0: initial BTEX concentration)

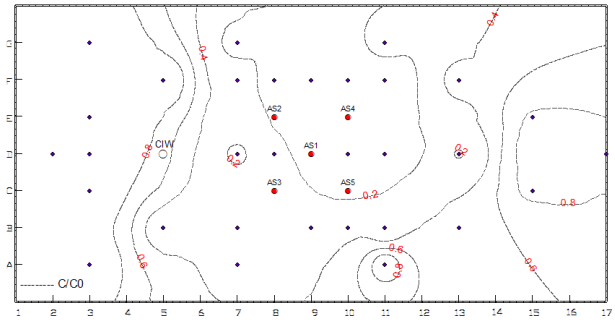

Fig. 13. Contour map of relative BTEX concentration, C/C_0, at the end of EX4 operation.

In order to compare the relation of DO, WL change and BTEX removal during AS experiments, Fig. 14 is presented. The results of EX1 and EX3 experiments are plotted in Fig. 14(a) as maximum DO change vs. maximum BTEX removal and in Fig. 14(b) as maximum WL change vs. maximum BTEX removal of monitoring wells. Furthermore, the results of EX2 and EX4 experiments are plotted in Fig. 14(c) as maximum DO change vs. maximum BTEX removal and in Fig. 14(d) as maximum WL change vs. maximum BTEX removal of monitoring wells. Figs. 14(a) and (c) shows that the monitoring wells that have significant DO change have also significant BTEX removal. Therefore, there was a relatively sound correlation between DO change (indirect indicator) and BTEX removal

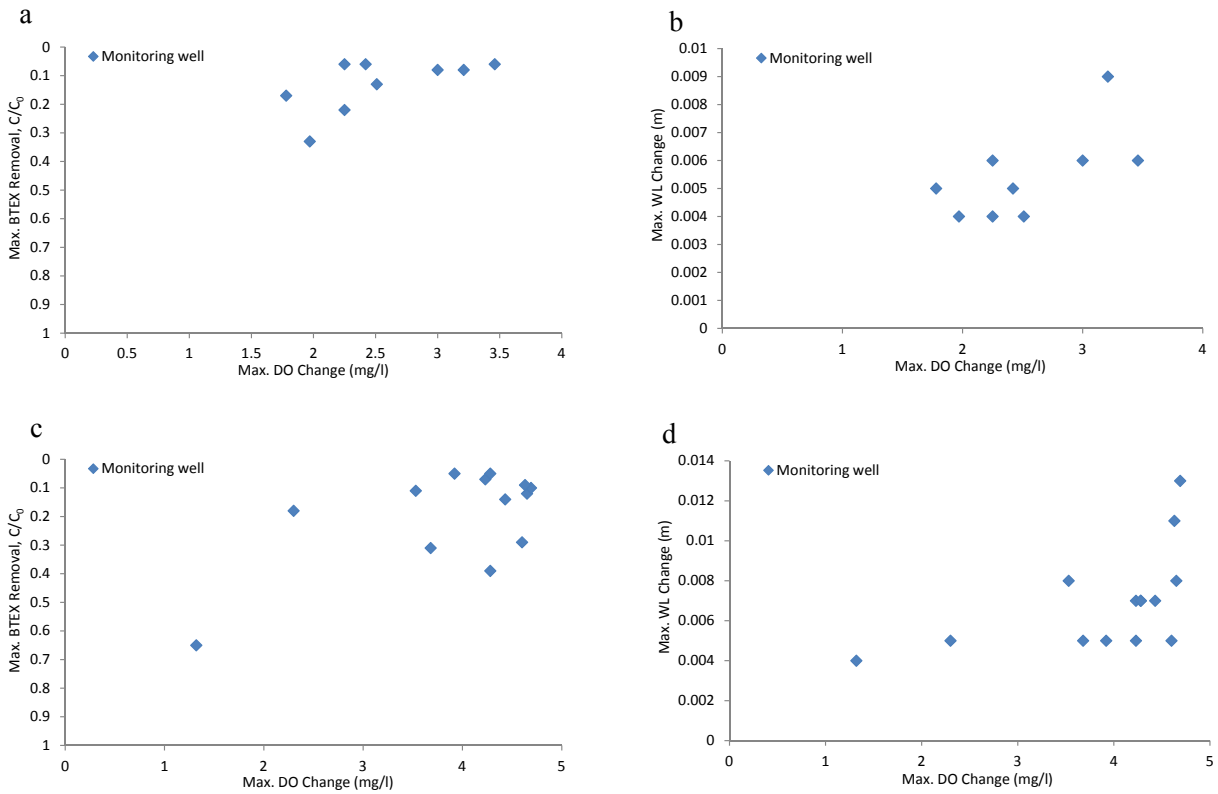

Fig. 14. DO, water level change and BTEX removal relation during AS experiments; (a) and (b): during single well sparging strategy (EX1 and EX3) and (c) and (d): during the multi-well sparging strategy (EX2 and EX4).

(direct indicator of sparging well ROI) during AS experiments. While Figs. 14(b) and (d) show that there is not a good correlation between WL change and BTEX removal.

4. Summary and conclusions

Laboratory treatability study is helpful to evaluate the effectiveness of a selected remediation method in reaching remedial goal and provides some understandings of the complex processes and design parameters for the site-specific condition. In this study to evaluate the efficiency of the AS method for BTEX removal in the "fine-grained" material and "specific hydrogeological condition" of SOR site, a lab-scale 3-D box model is used. A series of experiments were conducted, and the followings were concluded or recommended for a successful IAS operation.

AS remediation method is effective to reduce BTEX concentration in fine-grained material of SOR aquifer if well designed and operated. Since the removal rate of BTEX decreases with time during the operation for a constant rate of airflow, changing the sparging strategy such as pulsing could be a more efficient operation.

Increasing the sparging flow rate can result in increasing the BTEX removal to some extent, but not necessarily increases the sparging wells ROI, especially in the fine-grained porous materials that channelling is a dominant airflow mode. Therefore, for the SOR fine-grained porous media, multi air injection point with lower sparging flow rate strategy is more effective.

The most important parameter in AS design is recognition of ROI of the sparging well. Contaminant cleanup zone (as direct indicator of ROI) best defines the sparging well ROI. Results indicated a corresponding of DO concentration and BTEX removal zone. As hydrocarbon analysis is expensive, sparging well ROI can be inferred from DO measurements (as indirect indicator of ROI) during the AS operation.

In fine-grained material that channelized flow is dominant, determination of sparging well ROI is ambiguous. In our study interest phenomena was observed in monitoring wells that had less distance to sparging point but less BTEX removal rate or less DO value change in respect to wells with more distance to sparging point. Probably air flowed in discrete meandering channels mode. The monitoring wells located on individual channel can lead to over estimation of the ROI, while, there are areas between channels that have not affected by induced air. Therefore, in fine-grained porous material special consideration in determining ROI is required by proper design of number and placement of monitoring points.

When air injected through single sparging well with $(10 \pm 1) \times 10^3$ cm^3/min airflow rate for first 24 h, there were observed some fundamental limitation associated with AS efficiency due to air channeling. Doubling the airflow rate $((20 \pm 1) \times 10^3$ cm^3/min for next 24 h) did not improved AS efficiency significantly. Channelling is most probable airflow mode during AS experiment in fine-grained aquifer of SOR as expected. The location, number and density of air channels will influence the ability of the sparging system to volatilize contaminants. At

the individual channel or its vicinity, the rate of contaminant recovery may be rapid as contaminant in the immediate vicinity of air channels is in direct contact with induced air; however, for contaminants out of air channels, there is a diffusion limitation to volatilize into the air channels. The presence of diffusion limitations may severely affect the efficiency of AS. Therefore, channelling is a removal rate-limiting factor, and so AS remediation can be less effective or not effective in the fine-grained aquifers. Although channelling is a removal rate-limiting factor and reduces AS effectiveness in fine-grained material, but results of study indicated that by some considerations such as decreasing airflow rate and increasing number of spaging points, this limitation could be relaxed and increases AS range of applicability in fine-grained porous material. Therefore, the result of this study proposed a beneficial strategy during AS application to overcome the limitation of AS remediation technology in fine-grained aquifers such as SOR.

Acknowledgments

We thank the Iran National Science Foundation (INSF) for supporting some project expenses. Many thanks to Fatemeh Damercheli and Ashrafossadat Mousavi of the Iranian Mineral Processing Research Center (IMPRC) for analyzing the water samples. We acknowledge Shiraz University for providing the facilities to work on this research project.

References

[1] C.M. Kao, J. Prosser, Evaluation of natural attenuation rate at a gasoline spill site, J. Hazard. Mater., 82 (2001) 275–289.
[2] A.E. Stricker, H. Lossing, J.H. Gibson, Y. Hong, J.C. Urbanic, Pilot-scale testing of a new configuration of the membrane aerated biofilm reactor (MABR) to treat high-strength industrial sewage, Water Environ. Res., 83 (2011) 3–14.
[3] C.P. Ardito, J.F. Billings, Alternative Remediation Strategies: The Subsurface Volatilization and Ventilation System, Proc. Petroleum Hydrocarbons and Organic Chemicals in Groundwater: Prevention, Detection, and Restoration Conference, National Groundwater Association, Dublin, OH, 1990, pp. 281–296.
[4] M.C. Marley, D.J. Hazebrouck, M.T. Walsh, The application of in situ air sparging as an innovative soils and groundwater remediation technology, Ground Water Monit. Remediat., 12 (1992) 137–145.
[5] W.C. Leonard, R.A. Brown, Air Sparging: An Optimal Solution, Proc. Petroleum Hydrocarbons and Organic Chemicals in Groundwater: Prevention, Detection, and Restoration Conference, National Groundwater Association, Dublin, OH, 1992, pp. 349–363.
[6] R.L. Johnson, P.C. Johnson, D.B. McWhorter, R.E. Hinchee, I. Goodman, An overview of in situ air sparging, Ground Water Monit. Remediat., 13 (1993) 127–135.
[7] K.R. Reddy, S. Kosgi, J. Zhou, A review of in-situ air sparging for the remediation of VOC-contaminated saturated soils and groundwater, Hazard. Waste Hazard. Mater., 12 (1995) 97–118.
[8] W.S. Clayton, A field and laboratory investigation of air fingering during air sparging, Ground Water Monit. Remediat., 18 (1998) 134–145.
[9] J.A. Adams, K.R. Reddy, Removal of dissolved and NAPL–phase benzene pools from groundwater using in-situ air sparging, J. Environ. Eng., 126 (2000) 697–707.
[10] R.E. Hinchee, Air Sparging for Site Remediation, Lewis Publishers/CRC Press, Boca Raton, FL, 1994, pp. 38–55.
[11] U.S. Environmental Protection Agency (EPA), How to Evaluate Alternative Cleanup Technologies for Underground Storage Tank Sites: A Guide for Corrective Action Plan Reviewers, 2004, EPA 510-R-04-002.
[12] W. Ji, A. Dahmani, D.P. Ahlfeld, J.D. Lin, E. Hill, Laboratory study of air sparging: airflow visualization, Ground Water Monit. Remediat., 13 (1993) 115–126.
[13] K.R. Reddy, J.A. Adams, System effects on benzene removal from saturated soils and ground water using air sparging, J. Environ. Eng. 124 (1998) 288–299.
[14] S.W. Rogers, S.K. Ong, Influence of porous media, airflow rate, and air channel spacing on benzene NAPL removal during air sparging, Environ. Sci. Technol., 34 (2000) 764–770.
[15] J.W. Peterson, M.J. DeBoer, K.L. Lake, A laboratory simulation of toluene cleanup by air sparging of water-saturated sands, J. Hazard. Mater., 72 (2000) 167–178.
[16] K.R. Reddy, J.A. Adams, Effects of soil heterogeneity on airflow patterns and hydrocarbon removal during in situ air sparging, J. Geotech. Geoenviron. Eng., 127 (2001) 234–247.
[17] G. Heron, J.S. Gierke, B. Faulkner, S. Mravik, L. Wood, C.G. Enfield, Pulsed air sparging in aquifers contaminated with dense nonaqueous phase liquids, Ground Water Monit. Remediat., 22 (2002) 73–82.
[18] W.A.P. Waduge, K. Soga, J. Kawabata, Effect of NAPL entrapment conditions on air sparging remediation efficiency, J. Hazard. Mater., 110 (2004) 173–183.
[19] Y.J. Tsai, Y.C. Kuo, T.C. Chen, Groundwater remediation using a novel micro-bubble sparging method, J. Environ. Eng. Manage., 17 (2007) 151–155.
[20] L. Hu, X. Wu, Y. Liu, J.N. Meegoda, S. Gao, Physical modeling of air flow during air sparging remediation, Environ. Sci. Technol., 44 (2010) 3883–3888.
[21] C.Y. Qin, Y.S. Zhao, Y. Su, W. Zheng, Remediation of non-aqueous phase liquid polluted sites using surfactant-enhanced air sparging and soil vapor extraction, Water Environ. Res., 85 (2013) 133–140.
[22] C.Y. Qin, Y.S. Zhao, L.L. Li, W. Zheng, Mechanisms of surfactant-enhanced air sparging in different media, J. Environ. Sci. Health., Part A, 48 (2013) 1047–1055.
[23] C.Y. Qin, Y.S. Zhao, L.L. Li, W. Zheng, The influence zone of surfactant-enhanced air sparging in different media, Environ Technol., 35 (2014) 1190–1198.
[24] M.W. Kresge, M.F. Dacey, An Evaluation of *In Situ* Groundwater Aeration, Presented at Hazardous Waste Materials Management Conference, Atlantic City, NJ, 1991.
[25] R.A. Brown, F. Jasiulewicz, Air sparging: a new model for remediation, Pollut. Eng., 7 (1992) 52–55.
[26] D.W. Felten, M.C. Leahy, L.J. Bealer, B.A. Kline, Case study: site remediation using air sparging and soil vapor extraction, Proc. Petroleum Hydrocarbons and Organic Chemicals in Groundwater: Prevention, Detection, and Restoration Conference, National Ground Water Association, Dublin, OH, 1992, pp. 395–411.
[27] M.E. Loden, A Technology Assessment of Soil Vapor Extraction and Air Sparging, U.S. Environmental Protection Agency, Office of Research and Development, Washington, DC, 1992, EPA/600/R-92/173.
[28] E.K. Nyer, S.A. Sutherson, Air sparging: savior of groundwater remediations or just blowing bubbles in the bath tub? Ground Water Monit. Remediat., 13 (1993) 87–91.
[29] S. Gao, J.N. Meegoda, L. Hu, Microscopic modeling of air migration during air sparging, J. Hazard. Toxic Radioact. Waste, 15 (2011) 70–79.
[30] S. Gao, J.N. Meegoda, L. Hu, A dynamic two-phase flow model for air sparging, Int. J. Numer. Anal. Methods Geomech., 37 (2013) 1801–1821.
[31] L. Hu, J. Meegoda, J. Du, S. Gao, X. Wu, Centrifugal study of zone of influence during air-sparging, J. Environ. Monit., 13 (2011) 2443–2449.
[32] L. Hu, J. Meegoda, H. Li, J. Du, S. Gao, Study of flow transitions during air sparging using the geotechnical centrifuge, J. Environ. Eng., 141 (2015) 04014048-1–04014048-8. doi: 10.1061/(ASCE) EE.1943-7870.0000877
[33] Y. Ansari, G. Habibagahi, Modeling of LNAPL Spreading and Migration to Locate the Source and Fate of Oil Leaks, Presented at the 7th International Congress on Civil Engineering, Tehran, Iran, 2004.

[34] A. Vaezihir, M. Zare, E. Raeisi, J. Molson, J. Barker, Field-scale modeling of benzene, toluene, ethylbenzene, and xylenes (BTEX) released from multiple source zones, Biorem. J., 16 (2012) 156–176.
[35] M.M. Martinson, J.A. Linck, Field Pilot-Testing for Air Sparging of Hydrocarbon-Contaminated Groundwater, Proc. Sixteenth International Madison Waste Conference, University of Wisconsin-Madison, 1993.
[36] G. Mickelson, Guidance for Design, Installation and Operation of In-Situ Air Sparging Systems, Wisconsin Department of Natural Resources, Emergency and Remedial Response Section, Publication Number: PUBL-SW186-93, 1993.
[37] D.P. Ahlfeld, A. Dahmani, W. Ji, A conceptual model of field behavior of air sparging and its implications for application, Ground Water Monit. Remediat., 14 (1994) 132–139.